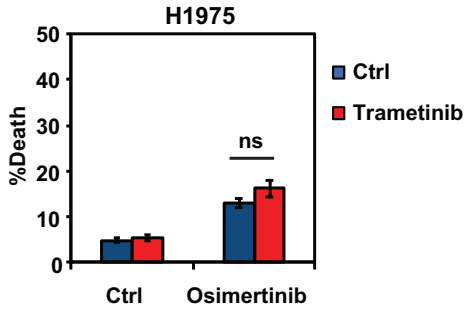

Figure S1. Related to Figure 1. Trametinib has a minimal impact on osimertinib-induced apoptosis. H1975 cells were treated with the indicated agents (2 μM) for 48 h. Cell death was quantified by annexin-V staining (mean ± s.d., n=3).

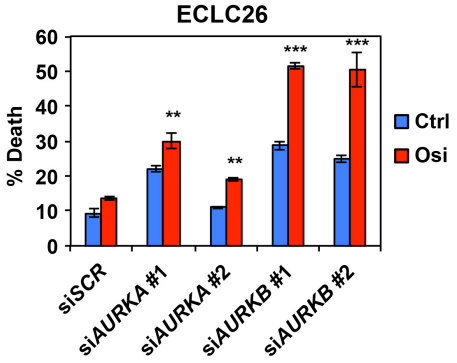

Figure S2. Related to Figure 2. KD of *AURKB* has a greater impact than KD of *AURKA* on osimertinib-induced apoptosis. ECLC26 cells transfected with the indicated siRNAs for 24 h were treated with vehicle or osimertinib (2 μM) for 24 h. Cell death was quantified by annexin-V staining (mean ± s.d., n=3). **, $P<0.01$; ***, $P<0.001$ (Student's *t*-test).

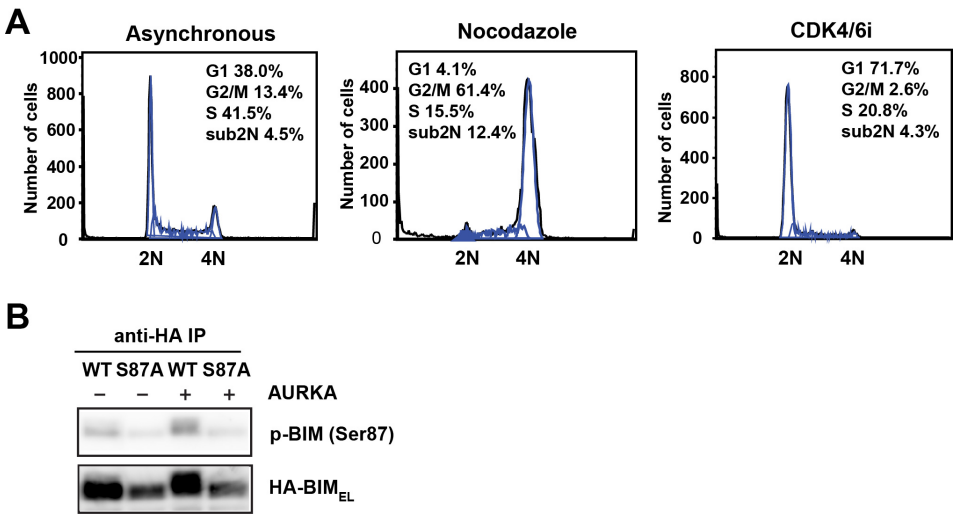

Figure S3. Related to Figure 3. Cell cycle profiling and *in vitro* AURKA kinase assays. (A) H1975 cells treated with nocodazole for 16 h or palbociclib for 24 h were subjected to cell-cycle analysis using propidium iodide staining. Cell-cycle phase distribution was quantified by the FlowJo software. (B) The *BAX*$^{-/-}$*BAK*$^{-/-}$ H1975 cells stably expressing HA-tagged WT BIM or BIM S87A mutant as described in Figure 3G were treated with palbociclib (1 μM) for 24 h and subjected to anti-HA immunoprecipitation. The immunoprecipitates were incubated with recombinant Aurora A kinase in the presence of ATP. The kinase reaction products were assessed by immunoblots using antibodies against p-BIM on Ser87 or BIM.

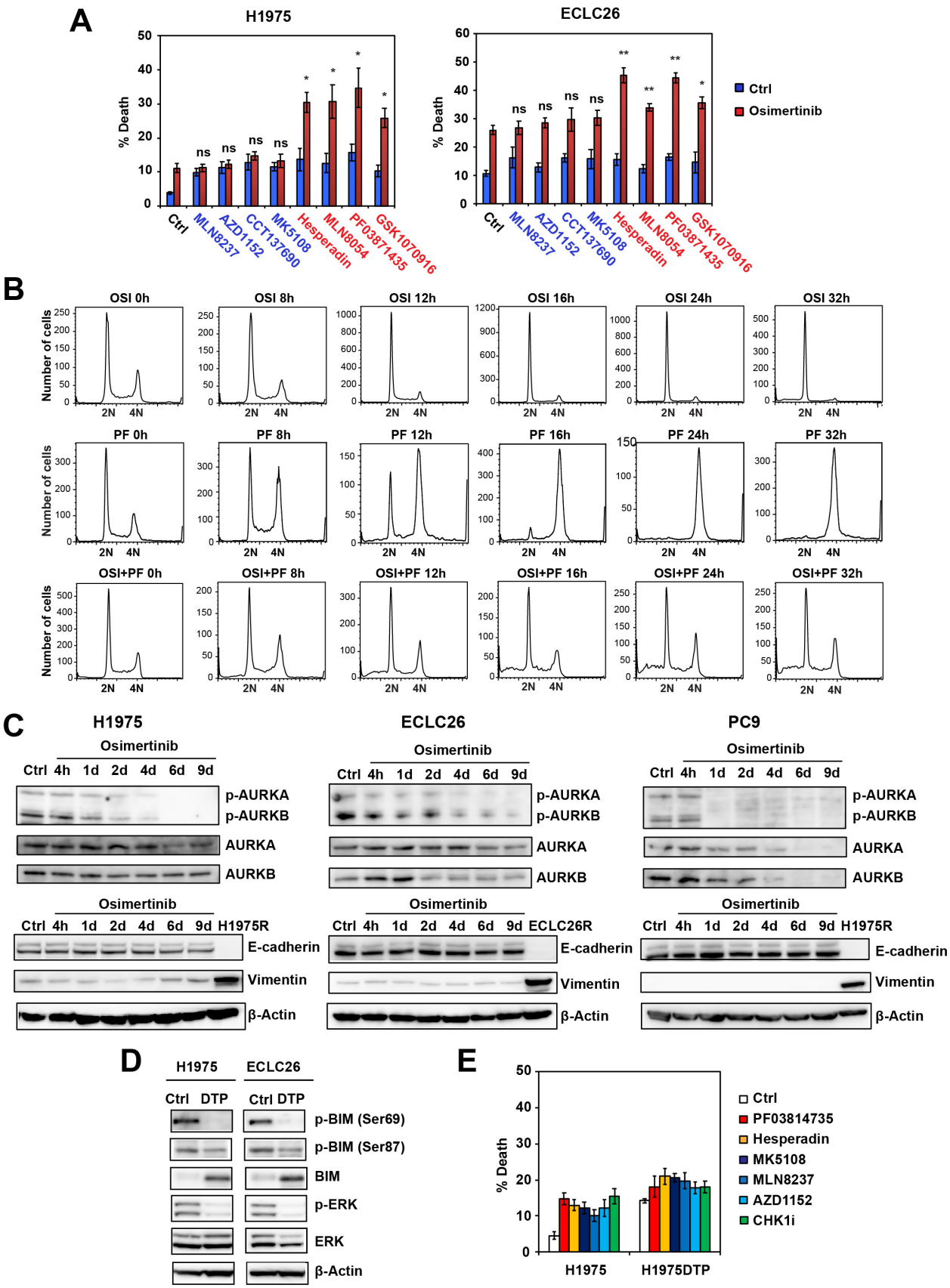
A
H1975
ECLC26
% Death
Ctrl
Osimertinib
ns
Ctrl
MLN8237
AZD1152
CCT137690
MK5108
Hesperadin
MLN8054
PF03871435
GSK1070916
B
OSI 0h
OSI 8h
OSI 12h
OSI 16h
OSI 24h
OSI 32h
PF 0h
PF 8h
PF 12h
PF 16h
PF 24h
PF 32h
OSI+PF 0h
OSI+PF 8h
OSI+PF 12h
OSI+PF 16h
OSI+PF 24h
OSI+PF 32h
Number of cells
2N
4N
C
H1975
ECLC26
PC9
Osimertinib
Ctrl 4h 1d 2d 4d 6d 9d
p-AURKA
p-AURKB
AURKA
AURKB
H1975R
ECLC26R
E-cadherin
Vimentin
β-Actin
D
H1975
ECLC26
Ctrl DTP
p-BIM (Ser69)
p-BIM (Ser87)
BIM
p-ERK
ERK
β-Actin
E
% Death
Ctrl
PF03814735
Hesperadin
MK5108
MLN8237
AZD1152
CHK1i
H1975
H1975DTP

Figure S4. Related to Figure 4. Cell death, cell cycle, and immunoblot analyses. (A) H1975 and ECLC26 cells were treated with the indicated Aurora kinase inhibitors (0.5 μM) ± osimertinib (2 μM) for 48 h. Cell death was quantified by annexin-V staining (mean ± s.d., n=3). *, $P<0.05$; **, $P<0.01$ (Student's *t*-test). (B) H1975 cells were treated with osimertinib (1 μM) and/or PF03814735 (1 μM) and subjected to cell-cycle analysis using propidium iodide staining at the indicated times. Cell-cycle phase distribution was quantified by the FlowJo software. (C) H1975, ECLC26, and PC9 cells treated with osimertinib (1 μM) for the indicated times were subjected to immunoblot analyses. (D) H1975, ECLC26, and drug-tolerant persisters (DTPs) of H1975 or ECLC26 following osimertinib (1 μM) treatment for 9 days were subjected to immunoblot analyses. (E) H1975 and H1975DTP cells were treated with the indicated agents (0.5μM) for 48h. Cell death was quantified by annexin-V staining (mean ± s.d., n=3).

A

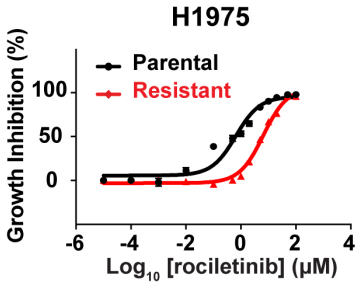

H1975	Parental	Resistant
EC50 (μM)	0.6532	6.543

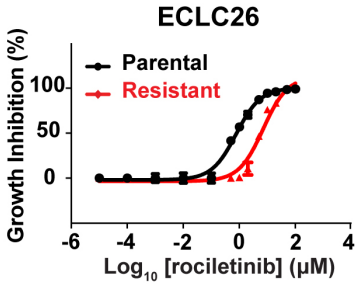

ECLC26	Parental	Resistant
EC50 (μM)	0.7762	7.123

B

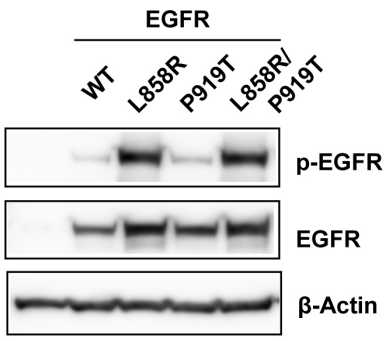

C

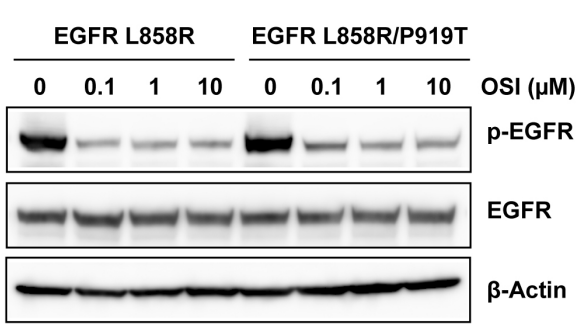

D

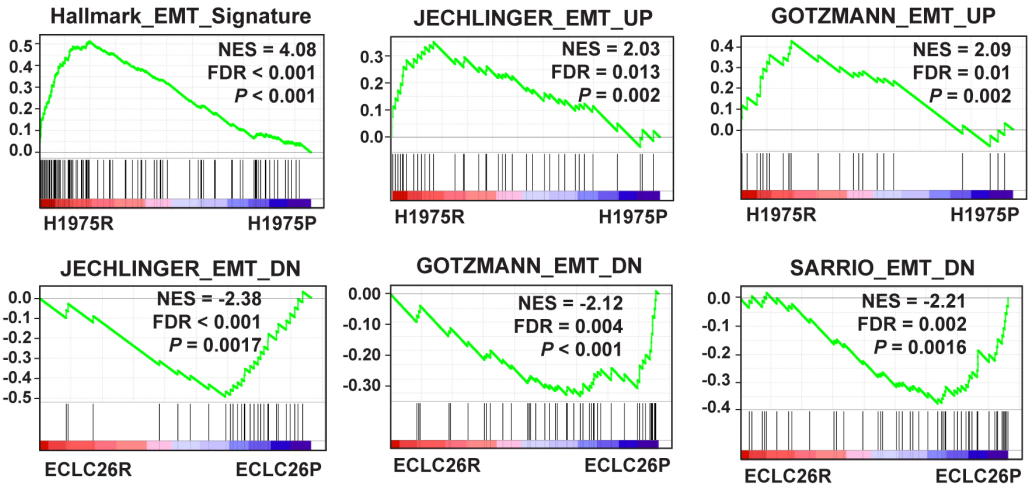

E

Compound	Target	H1975P EC50 (μM)	H1975R EC50 (μM)	Ratio	ECLC26P EC50 (μM)	ECLC26R EC50 (μM)	Ratio
PF03814735	Aurora kinase	2.27	0.93	2.45	34.10	2.53	13.47
MLN8054	Aurora kinase	6.07	1.05	5.78	12.25	2.68	4.57
GSK1838705A	IGF1R	5.82	4.28	1.36	9.99	5.20	1.92
NVP-AEW541	IGF1R	7.95	5.31	1.50	5.37	3.10	1.73
Rebastinib	SRC family kinases	2.13	2.17	0.98	2.42	0.87	2.80
Sarcatinib	SRC family kinases	20.15	16.70	1.21	0.43	10.61	0.04

Figure S5. Related to Figure 5. Comparison of parental and osimertinib-resistant H1975 or ECLC26 cells. (A) The parental as well as osimertinib-resistant H1975 and ECLC26 cells were treated with rociletinib at the indicated concentrations. Cell viability was assessed by CellTiter-Glo assays at 72 h and EC50 was calculated. (B) EGFR P919T is not an activating mutation. NIH3T3 cells transduced with control retrovirus or retrovirus expressing wild-type EGFR, EGFR L858R, EGFR P919T, or EGFR L858R/P919T were assessed by immunoblot analyses. (C) EGFR P919T does not confer resistance to osimertinib. NIH3T3 cells transduced with retrovirus expressing EGFR L858R or EGFR L858R/P919T were treated with the indicated concentrations of osimertinib for 2h and assessed by immunoblot analyses. (D) GSEA plots of the differentially expressed genes (FDR < 0.05) comparing parental with osimertinib-resistant H1975 or ECLC26 cells using the indicated EMT signatures. (E) Summary of EC50 of the indicated agents in the parental as well as osimertinib-resistant H1975 and ECLC26 cells. The ratio of EC50 in the parental cells compared to that of osimertinib-resistant cells was calculated.

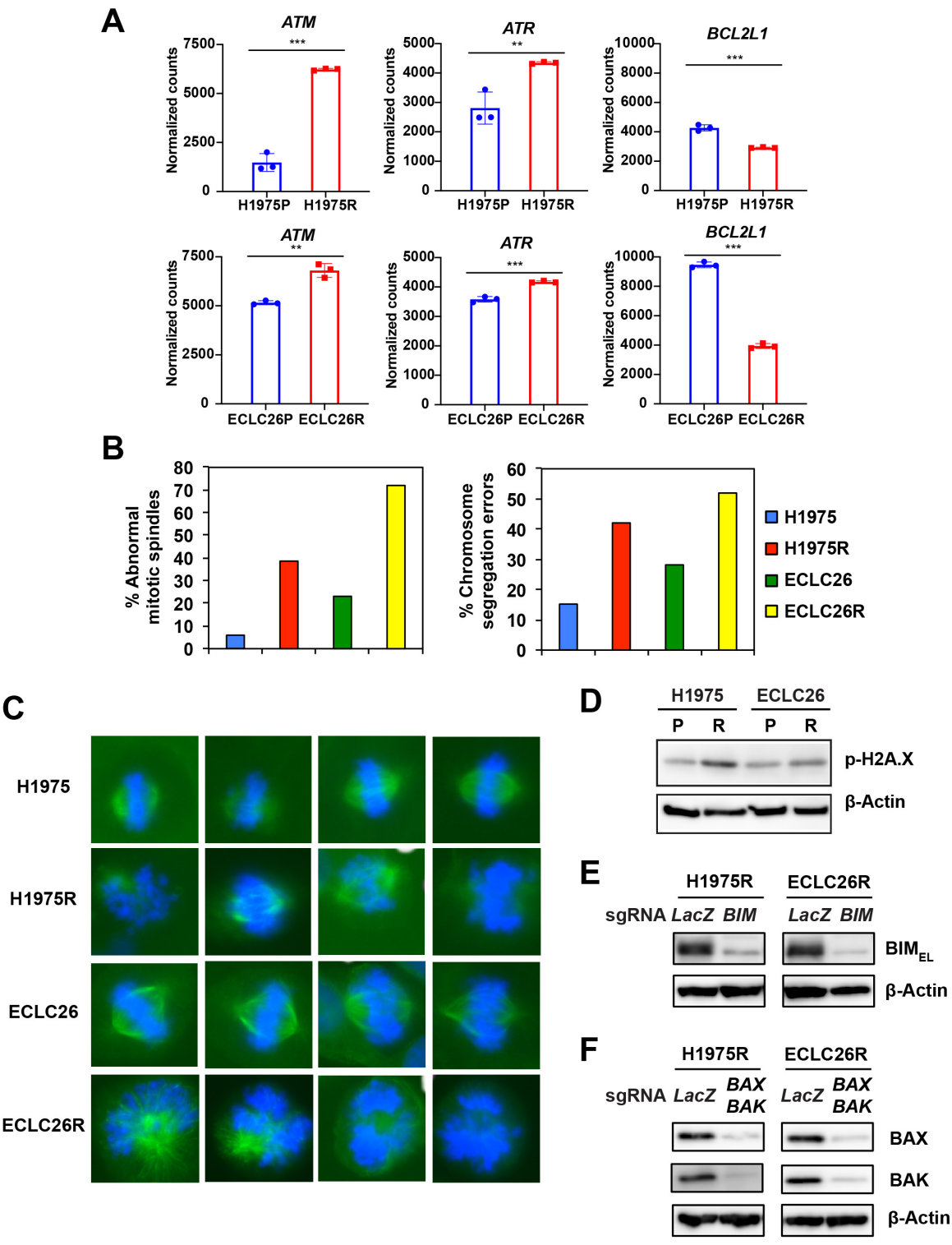
A
ATM
ATR
BCL2L1
Normalized counts
H1975P H1975R
ECLC26P ECLC26R
B
% Abnormal mitotic spindles
% Chromosome segregation errors
H1975
H1975R
ECLC26
ECLC26R
C
H1975
H1975R
ECLC26
ECLC26R
D
H1975 ECLC26
P R P R
p-H2A.X
β-Actin
E
H1975R ECLC26R
sgRNA LacZ BIM LacZ BIM
BIM$_{EL}$
β-Actin
F
H1975R ECLC26R
sgRNA LacZ BAX BAK LacZ BAX BAK
BAX
BAK
β-Actin

Figure S6. Related to Figure 6. Analyses of RNA-seq and mitotic defects comparing osimertinib-resistant H1975 or ECLC26 cells with their parental counterparts. (A) Analysis of RNA-seq data shows upregulation of *ATM* and *ATR* and downregulation of *BCL-X_L* in both H1975R and ECLC26R cells compared to their parental counterparts (H1975P and ECLC26P). (B) Assessment of mitotic defects based on α-tubulin (microtubules) immunostaining in the indicated cell lines. Shown are the percentage of counted cells ($n \geq 50$) with abnormal microtubule spindle geometry and chromosome segregation errors. (C) Representative immunofluorescence images from two independent experiments in the indicated cell lines. Green, α-tubulin immunostaining; blue, Hoechst staining of DNA. (D) The indicated cells were assessed by immunoblots. (E) H1975R and ECLC26R cells transduced with lentivirus expressing sgRNAs targeting *LacZ* or *BIM* were subjected to immunoblot analyses. (F) H1975R and ECLC26R cells transduced with lentivirus expressing sgRNAs targeting *LacZ* or *BAX and BAK* were subjected to immunoblot analyses.

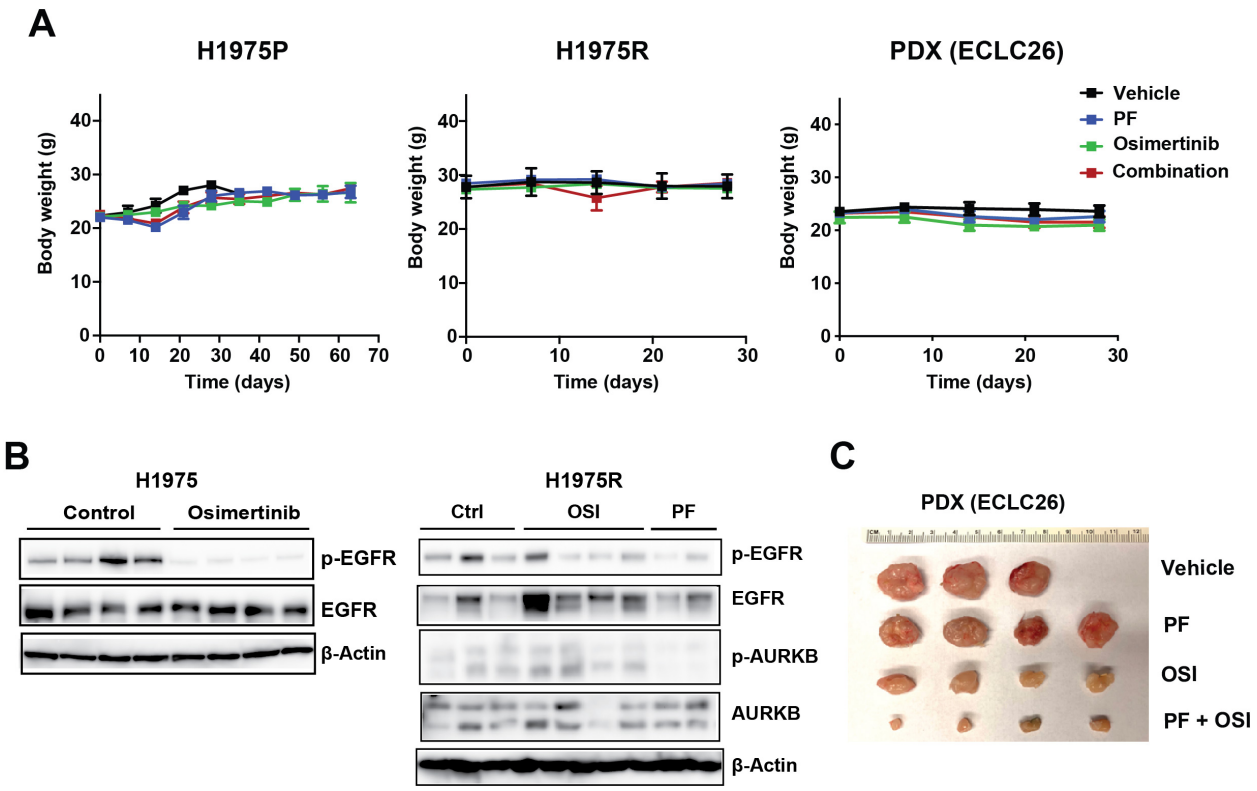

Figure S7. Related to Figure 7. *EGFR*-mutant lung cancer xenograft studies. (A) Changes in body weight for mice bearing xenografts derived from H1975P or H1975R as well as patient-derived xenografts (ECLC26) treated with vehicle, osimertinib (5 mg/kg), PF03814735 (20 mg/kg), or the combination. (B) Immunoblot analyses of lysates from H1975 or H1975R xenograft tumors harvested following the treatment with the indicated agents. (C) Representative gross images of patient-derived xenograft tumors from mice treated with the indicated agents for 28 days.

Table S2. **Related to Figure 5**. Development of osimertinib resistance in H1975 cells results in upregulation as well as downregulation of several hallmark signatures revealed by GSEA (H: hallmark gene sets).

NAME	NES	NOM p-val	FDR q-val
HALLMARK_EPITHELIAL_MESENCHYMAL_TRANSITION	4.079	0.000	0.000
HALLMARK_UV_RESPONSE_DN	2.607	0.000	0.000
HALLMARK_ANGIOGENESIS	2.120	0.002	0.005
HALLMARK_MYOGENESIS	1.886	0.000	0.017
HALLMARK_INTERFERON_ALPHA_RESPONSE	-2.307	0.000	0.001
HALLMARK_INTERFERON_GAMMA_RESPONSE	-2.250	0.000	0.001
HALLMARK_ESTROGEN_RESPONSE_EARLY	-2.156	0.000	0.002
HALLMARK_KRAS_SIGNALING_UP	-2.101	0.000	0.003
HALLMARK_ESTROGEN_RESPONSE_LATE	-1.905	0.000	0.021
HALLMARK_APICAL_JUNCTION	-1.905	0.003	0.018
HALLMARK_APICAL_SURFACE	-1.838	0.011	0.024
HALLMARK_E2F_TARGETS	-1.798	0.005	0.028
HALLMARK_ALLOGRAFT_REJECTION	-1.771	0.007	0.030
HALLMARK_GLYCOLYSIS	-1.683	0.015	0.050
HALLMARK_KRAS_SIGNALING_DN	-1.598	0.029	0.081
HALLMARK_ANDROGEN_RESPONSE	-1.591	0.049	0.076
HALLMARK_MYC_TARGETS_V1	-1.536	0.050	0.091

Table S3. **Related to Figure 6**. Analysis of correlations between mRNA levels of the indicated genes from *EGFR*-mutant LUAD in TCGA (n = 25). R, Pearson correlation coefficient; FDR *q*-value by the Benjamini-Hochberg method.

***EGFR*-mt LUAD (N=25), R/q-value**

	FOXA1	FOXA2	ZEB1	ZEB2
ATR	0.071/0.368	-0.066/0.378	0.275/0.092	0.591/0.001
ATM	0.065/0.379	-0.068/0.374	-0.011/0.480	0.127/0.273
VIM	-0.286/0.083	-0.209/0.158	0.558/0.002	0.383/0.029
CDH1	-0.057/0.393	0.319/0.060	-0.001/0.499	-0.183/0.190

Table S4. **Related to Figure 6**. Analysis of correlations between mRNA levels of the indicated genes from TCGA-LUAC cohort (n = 230). R, Pearson correlation coefficient; FDR *q*-value by the Benjamini-Hochberg method.

LUAD (N=230), R/q-value

	FOXA1	FOXA2	ZEB1	ZEB2
ATR	0.065/0.481	-0.175/0.025	0.137/0.092	0.213/4.953e-3
ATM	-0.037/0.687	-0.047/0.600	0.365/1.36e-7	0.452/2.00e-11
VIM	-0.273/1.784e-4	-0.101/0.227	0.548/6.37e-17	0.524/2.14e-15
CDH1	0.165/0.892	0.090/0.351	0.054/0.607	0.021/0.862

Table S5. **Related to Figure 7**. Summary of mutations detected by MSK-IMPACT assays comparing pre-treatment *EGFR*-mutant lung tumors and the corresponding patient-derived xenografts derived during disease progression under osimertinib treatment.

Ru813c patient's metastatic tumor				
HUGO_Symbol	**Variant_Class**	**Amino_Acid_Change**	**T_Alt_Freq**	**T_Coverage**
EGFR	In_Frame_Del	E746_S752delinsV	0.12	483
NF2	Nonsense_Mutation	Q125*	0.14	428
ATM	Missense_Mutation	G134D	0.11	274
RARA	Missense_Mutation	F310V	0.09	558
Ru813c PDX				
HUGO_Symbol	**Variant_Class**	**Amino_Acid_Change**	**T_Alt_Freq**	**T_Coverage**
EGFR	In_Frame_Del	E746_S752delinsV	0.57	521
NF2	Nonsense_Mutation	Q125*	1	275
RARA	Missense_Mutation	F310V	0.49	1187
Lx1114 patient's primary tumor				
HUGO_Symbol	**Variant_Class**	**Amino_Acid_Change**	**T_Alt_Freq**	**T_Coverage**
EGFR	In_Frame_Del	E746_A750del	0.88	3945
TP53	Missense_Mutation	R280G	0.24	756
CCND2	Missense_Mutation	H162Y	0.21	590
EPHA5	Missense_Mutation	E754Q	0.25	332
Lx1114 PDX				
HUGO_Symbol	**Variant_Class**	**Amino_Acid_Change**	**T_Alt_Freq**	**T_Coverage**
EGFR	In_Frame_Del	E746_A750del	0.97	3953
TP53	Missense_Mutation	R280G	1	444
KEAP1	Missense_Mutation	p.G509R	0.95	396
CCND2	Missense_Mutation	H162Y	0.99	212
RTEL1	Missense_Mutation	p.V271M	0.52	486